Pergamon

Cement and Concrete Research 29 (1999) 561–565

CEMENT AND CONCRETE RESEARCH

Effect of loading on carbonation penetration in reinforced concrete elements

A. Castel *, R. François, G. Arliguie

Complesce Scientifique de Rangueil, I.N.S.A.—U.P.S. Genie Civil, Laboratoire Matériaux et durabilité des constructions (L.M.D.C.), 31077 Toulouse Cedex 4, France

Manuscript received 5 August 1998; accepted manuscript 20 January 1999

Abstract

Concrete tensile microcracking due to a mechanical loading enhances the diffusion of aggressive agents from concrete cover to the reinforcements, which leads to the beginning of the propagation period of steel corrosion. The purpose of this work is to quantify the effect of concrete microcracking on CO_2 penetration. Concrete carbonation was studied on two 13-year-old reinforced concrete beams subjected to atmospheric carbonation. Indeed, these beams were exposed to the climate of the south-west of France but in a covered place and were always stored in a loaded state. Because the microcracking network is quite impossible to characterise, the tensile stress in the reinforcements was chosen as the main parameter of the microcracking state. This investigation results on a proposed model whose accuracy predicts the increase of the carbonation depth of the concrete in relation to the tensile stress in rebar.

Keywords: Carbonation; Tensile properties; Reinforced concrete

The process of steel corrosion in real life of reinforced concrete can be modelled in four stages that take into account both service cracking and tensile microcracking [1]. As a result, cracks do not modify significantly the service life but tensile microcracking reduces the time that is necessary for aggressive agents to reach the reinforcement through the concrete cover. The quantification of this effect is essential to predict the service life of reinforced concrete structures. It is quite impossible to quantify the microcracking network in terms of density, width, and connectivity. Therefore, Konin and colleagues [2] characterised tensile microcracking in reinforced elements by using the tensile stress in steel rebar. This previous work was done in the case of chloride penetration and led to the introduction of a load function modifying the apparent diffusion coefficient. Another step to understanding the coupled mechanism of mechanical degradation and transport properties consists in studying carbonation.

The kinetics of the CO_2 penetration through concrete is often used to characterise the durability properties of the material because concrete carbonation is one of the major cause of reinforcement corrosion. Many research works have been carried out on this subject in order to quantify the effect of parameters such as concrete mix components and proportions, climatic conditions, cure duration, and formation of calcium carbonate [3–5]. However the influence of tensile concrete microcracking on the atmospheric CO_2 diffusion has still not been assessed in terms of quantification. Therefore the purpose of this work is to propose a correlation between the carbonation depth increase in a natural environment and the loading level of the reinforced concrete in tension directly representative of the concrete damage. This work is based on a long term experimental program, started in 1984 at the L.M.D.C., Toulouse [1]. The samples are reinforced concrete beams with different concrete covers. These beams are always stored in a loading state representative of the actual operating conditions of reinforced concrete structures.

1. Experimental program

1.1. Reinforced concrete specimens and conservation modes

The samples used for this study are two reinforced concrete beams with 15 × 28-cm cross section and 300-cm length with two different concrete covers, 1 cm and 4 cm (Fig. 1). The concrete composition is given in Table 1. The water content was adjusted to obtain 7 cm in slump test. The average compression stress obtained on cylinder specimens

* Corresponding author. Tel.: 33-05-61-55-99-33; Fax: 33-05-61-55-62-65; E-mail: arnaudcastel@insa-tlse.fr.

0008-8846/99/$–see front matter
PII: S0008-8846(99)00017-4

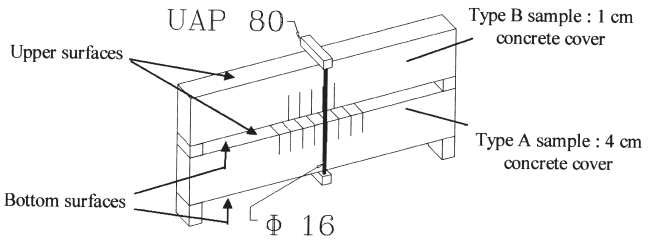

Fig. 1. Loading system in three points flexion.

was 45 MPa at 28 days. The construction of the beams was in compliance with current standards.

Both beams were exposed to a temperate climate (southwest of France) in a covered place since 1984. They were subjected to a carbonation due to atmospheric CO_2. The beams were loaded in three points flexion by coupling the A beam with the B beam. The A beam was thus in a back to front position compared with B sample position (Fig. 1). In spite of creeping, loading rates were kept constant by means of an adequate device. According to the French standards, the loading value (M_{ser} = 13.5 kN · m) corresponded to the maximum loading opposite durability for type A beam and to the maximum loading opposite resistance for type B element. The maximum stresses in the tensile reinforcements for A and B samples were 165 and 250 MPa, respectively.

No microcrack was found on the beams at the initial state before loading [6]. In the loading state, a diffuse tensile microcracking network was observed in the tensile zone of the reinforced concrete beams [7]. Microcracks were mainly located at interfacial transition zone and it was quite impossible to characterise the microcracking network.

1.2. Experimental method: Carbonation depth measurement

The method used to study carbonation measures the depth of neutralisation as indicated by a phenolphthalein solution sprayed on the newly fractured concrete surface. This indicator shows a magenta-coloured region on the concrete where the pH exceeds about 9 and a colourless area where the carbonation has reduced the pH to below 9.

The carbonation depth was measured along all tensile areas and all neutral fibers of both samples (about every 20 cm) respectively through cover concrete breaking and drilling of cores (Fig. 2). The measurements along the tensile area were made on the bottom and lateral surfaces of the type B beam and on the upper and the lateral surfaces of the type A sample (Fig. 1). Moreover, measurements were made far enough from the transversal macrocracks that usually appeared in regard to the stirrups, because the carbonation front was disrupted at their neighbourhood (Fig. 3).

2. Results and discussion

Figs. 4 and 5 show that for both samples the carbonation depth increases significantly in the tensile area in relation to the bending moment of the given cross section. Indeed, the increase of carbonation depth between the locations 20 and 140 cm on the lateral surface is about 35% for type A and 58% for type B samples (Table 2). The increase measured on type B beam is greater than the one obtained on type A element probably because the stress in the tensile reinforcements is greater for the B specimen. Fig. 6 shows concrete samples extracted along the tensile areas of both elements. As a result, on the 10-mm concrete cover beam, the carbonation front reaches the reinforcement in the middle area and consequently the propagation period of steel corrosion has started, whereas at 40 cm the reinforcements are still in a passive state. However, the carbonation front can be considered as being constant in the nonloaded fibres of the beams (and identical for both elements), with a value similar to the value obtained in the nonloaded cross sections in the tensile areas (location, 20 cm).

Moreover, the carbonation front measured on the lateral tensile surface is always deeper than the one obtained on the upper tensile surface for type A beam and on the bottom tensile surface for type B beam. Thus, for this type of conservation the lateral surfaces of a structural element are the most exposed to carbonation due to atmospheric CO_2. Indeed, on the upper surfaces moisture deposits probably hinder the penetration of the CO_2 and for the bottom surfaces the penetration is probably slowed in the vertical direction by the effect of the gravity.

Results show the influence of the tensile microcracking of the concrete on the CO_2 penetration. Since it is quite im-

Table 1
Concrete composition

Mix component							
Rolled gravel (silica + limestone)					5/15 mm	1220 kg/m^3	
Sand					0/5 mm	820 kg/m^3	
Portland cement high performance						400 kg/m^3	
Water						200 kg/m^3	
	Cement composition						
	SiO_2	AI_2O_3	Fe_2O_3	CaO	MgO	SO_3	Na_2O
% weight	21.4	6	2.3	63	1.4	3	0.5

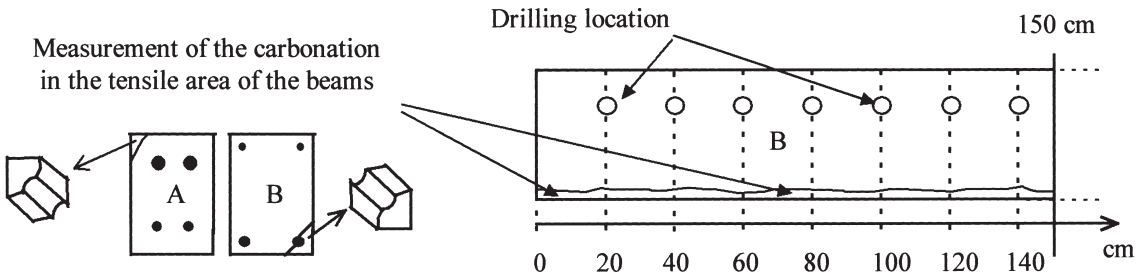

Fig. 2. Measurement of the carbonation depth along the beams.

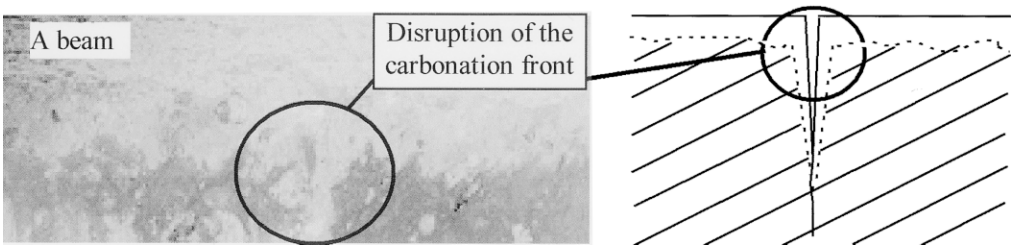

Fig. 3. Carbonation front at the neighbourhood of the service cracks.

possible to characterise the microcracking network, the tensile stress in the reinforcements (σs) was chosen as the main parameter of the microcracking state. Moreover, σs is already used in civil engineering rules as a durability parameter to control the service crack width. Recent studies [1,8] indicated that service crack width had no influence on the corrosion process, but σs could be a durability criterion as a threshold microscopic damage of the concrete.

For a considered tensile surface of the samples, the carbonation depth is marked CD; the carbonation depth at the 20-cm position, corresponding to the nonloaded cross section in flexion, is marked CD_o. We use the ratio CD/CD_o to isolate the intrinsic effect of the microcracking damage of the material and to eliminate the influence of the moisture deposits and the gravity action previously mentioned. Fig. 7 shows the evolution of the ratio CD/CD_o along both samples in relation to σs for the lateral, upper, and bottom surfaces (σs is calculated using standard reinforced concrete calculations). A global relationship whose accuracy correlates the experimental points can be proposed :

$$CD(\sigma s) = CD_o \cdot (1 + L(\sigma s)). \quad (1)$$

L(σs) is a function of the load: $L(\sigma s) = k\sigma s^3$ with k = constant. The model of Eq. (1) is similar to the one proposed by other authors [3] on the evolution of the chloride apparent diffusion coefficient in relation to σs. However, the value of the constant k seems to be different for A and B beams: $L(\sigma s) = 1 \times 10^{-7}\ \sigma s^3$ for type A beam and $L(\sigma s) = 4.3 \times 10^{-8}\ \sigma s^3$ for type B sample.

The tensile reinforcement stress σs can be considered as an adequate parameter of the tensile load state of the concrete, but this parameter does not take into account the fact that the concrete covers of samples are different: 4 cm for type A beam and 1 cm for type B sample. Indeed, σs is representative of the tensile strains of the concrete at the steel-concrete interface but it is not representative of the concrete

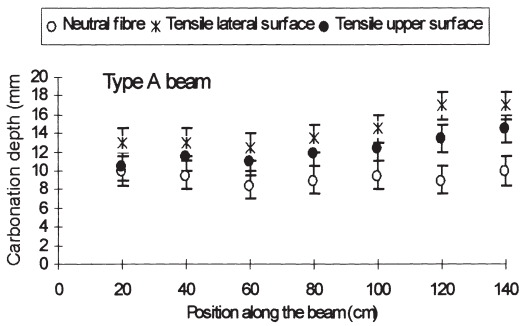

Fig. 4. Evolution of the carbonation front along the beam (type A beam).

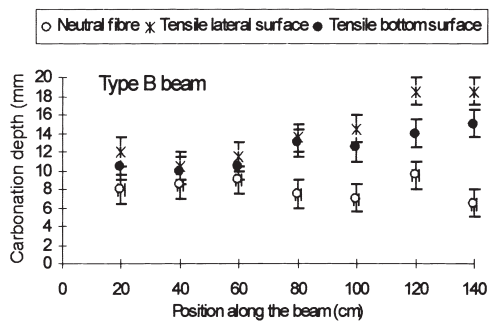

Fig. 5. Evolution of the carbonation front along the beam (type B beam).

Table 2
Carbonation depths (CD) in mm obtained on type A and B beams

The use of reinforced concrete specimens	20	40	60	80	100	120	140
Type A beam							
Neutral fibre	10	9.5	8.5	9	9.5	9	10
Tensile lateral surface	13	13	12.5	13.5	14.5	17	17
Tensile upper surface	10.5	11.5	11	12	12.5	13.5	14.5
Type B beam							
Neutral fibre	8	8.5	9	7.5	7	9.5	6.5
Tensile lateral surface	12	11	11.5	13.5	14.5	18.5	18.5
Tensile bottom surface	10.5	10	10.5	13	12.5	14	15

strains at the upper and bottom surfaces of the type A and type B beams that are in contact with atmospheric CO_2. These tensile strains increase as the concrete cover increases due to the curvature effect. To validate this assumption, concrete strain evolutions in the tensile area of another type A beam have been measured, using three strain gauges pasted at the concrete surface, far enough from the service cracks of the beam (Fig. 8). Gauge 1 measures the concrete strains along the tensile steels, gauge 3 measures the maximum concrete strains, and gauge 2 is in an intermediate position. The sample was subjected to a constant rate loading until the service loading value.

Results show that the tensile concrete strains recorded along the steels are significantly lower than the tensile concrete strains recorded by the gauges 2 and 3. Moreover, this difference increases when the distance between the steel location and the gauge position increases (Fig. 9). These results are in accordance with the assumption previously mentioned. In fact, there is a correlation between the three strains. Fig. 10 shows that the strains recorded by the gauges 2 and 3 are equal to those measured along the steels multiplied respectively by the ratios *h/x* and *h/d* (Fig. 8) where *d* is the effective depth. This allows us to consider another correlation model that takes into account the influence of the increase of the concrete cover on the maximum tensile strains of the concrete, due to the curvature effect. Indeed, the correction factor *h/d* is added to the value of σs in the model of Eq. (1) to derive Eq. (2):

$$CD(\sigma s) = CD_o \cdot \left[1 + \alpha \cdot \left(\frac{h \cdot \sigma s}{d}\right)^3\right] \quad (\alpha = \text{constant}) \quad (2)$$

Fig. 11 shows both curves of the model of Eq. (2) (the ratio *h/d* is equal to 1.25 for type A beam and 1.08 for type B element). The model seems to be accurately correlated to the experimental points obtained on both samples with a single value of the constant $\alpha = 4 \times 10^{-8}$ MPa−3 (for $\sigma s \leqslant 250$ MPa).

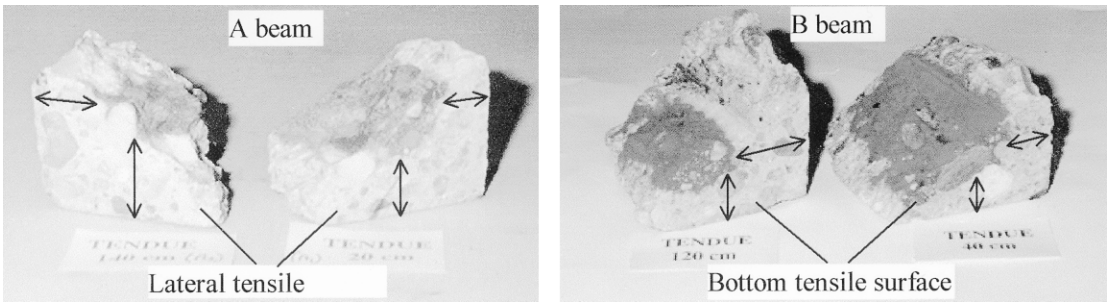

Fig. 6. Carbonation front obtained at the locations 140 and 20 cm of the type A sample and 120 and 40 of type B sample.

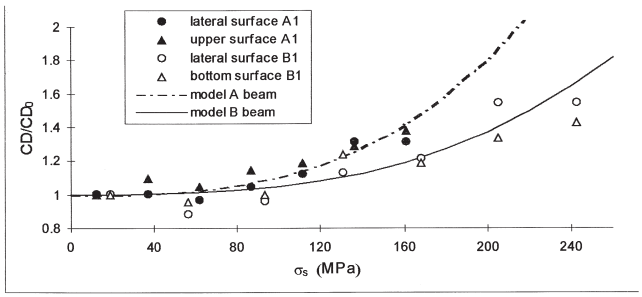

Fig. 7. Evolution of the carbonation depth in relation to σs.

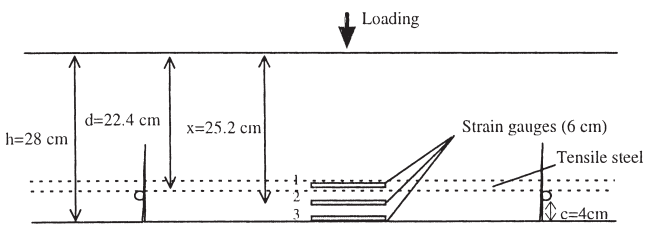

Fig. 8. Location of the strain gauges on the tensile area of a type A sample.

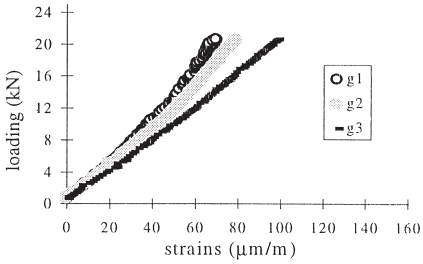

Fig. 9. Tensile concrete strains recorded on a type A sample.

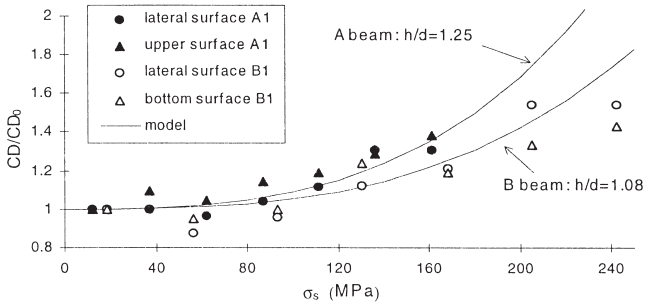

Fig. 11. Modelling of the evolution of the carbonation depth by Eq. (2).

3. Conclusions

The use of reinforced concrete specimens of large sizes and their storage under loading allows assessment of the real penetration of aggressive agents, such as atmospheric CO_2, and their influence on the corrosion process. Results show that the load applied to a reinforced concrete beam and its intensity play a significant role in the penetration of the CO_2 because of the increase of the tensile concrete microcracking mainly located at the paste-aggregate interface. The relationship proposed in this paper allows an accurate prediction of the increase of the carbonation depth using a tensile steel stress criterion (σs). Moreover, the model takes into account the curvature effect (structural elements loading in flexion) that influences the evolution of the carbonation depth for important concrete covers.

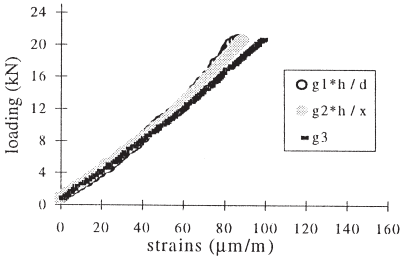

Fig. 10. Tensile concrete strains obtained after application of the correction factors.

References

[1] R. François, G. Arliguie, J.C. Maso, Annales de l'ITBTP 529 (1994) 1–48.
[2] A. Konin, R. François, G. Arliguie, Mater and Struct 31 (1998) 27–35.
[3] L.J. Parrott, Mater and Struct 29 (1996) 164–173.
[4] L.J. Parrott, Cem Concr Res 19 (1989) 649–656.
[5] L. Al-Akchar, V. Baroghel-bouny, A. Raharinaivo, First International Conference on Material Science and Concrete Properties, Toulouse, France, 1998, pp. 247–255.
[6] R. François , J.C. Maso, Annales de l'ITBTP 457 (1987) 50–56.
[7] R. François , J.C. Maso, Annales de l'ITBTP 464 (1988) 37–47.
[8] P. Schießl, M. Raupach, ACI Materials J 94 (1997) 56–62.